Journal of Organometallic Chemistry 694 (2009) 4140–4145

Contents lists available at ScienceDirect

Journal of Organometallic Chemistry

journal homepage: www.elsevier.com/locate/jorganchem

Acid/base sensitive platinum terpyridyl complex: Switching between metal-to-ligand charge transfer (MLCT), ligand-to-ligand charge transfer (LLCT), and intraligand charge transfer (ILCT) states

Zhiqiang Ji, Yunjing Li, Wenfang Sun *

Department of Chemistry and Molecular Biology, North Dakota State University, ND 58108-6050, USA

ARTICLE INFO

Article history:
Received 14 July 2009
Received in revised form 5 September 2009
Accepted 7 September 2009
Available online 11 September 2009

Keywords:
Platinum terpyridyl complex
Electronic absorption
Emission
Acid/base sensor
Metal-to-ligand charge transfer
Ligand-to-ligand charge transfer

ABSTRACT

A platinum(II) 2,2′:6′,2″-terpyridyl complex (**2**) with a hydroxylphenyl substituent on the terpyridyl ligand and a dimethylamino substituent on the phenylacetylide ligand was synthesized and characterized. Complex **2** exhibits a metal-to-ligand charge transfer (^{1}MLCT) absorption band at *ca.* 410 nm and a ligand-to-ligand charge transfer (^{1}LLCT) band at *ca.* 536 nm. It exhibits dual emission at *ca.* 450 nm and *ca.* 560 nm at room temperature when excited at 334 nm, which originates from the $^1\pi,\pi^*$ state and the ^{3}MLCT/$^3\pi,\pi^*$ state, respectively. Dramatic color change was observed for **2** with addition of acid and base. Its emission at 560 nm was enhanced in acidic solution and quenched in basic solution. The changes in absorption and emission could be attributed to the variation of the nature of the lowest excited state from LLCT to MLCT in acidic solution and to LLCT/ILCT at basic solution. The drastic color and emission intensity changes in acidic and basic solutions suggest that **2** could potentially be a colorimetric and luminescent acid/base sensor.

1. Introduction

Square-planar platinum(II) complexes have attracted a great interest in recent years due to their intriguing spectroscopic properties and potential applications in a variety of photonic devices, such as in organic light emitting diodes [1–9], photovoltaic cells [10–13], as nonlinear optical materials [14–19], photosensitizers [20–23], and chemical and biological sensors [24–30]. Platinum terpyridyl phenylacetylide complexes are particularly interesting because of their ease of synthesis and structural modifications. Upon structural modifications, the nature of the lowest excited state of these complexes can be tuned among the metal-to-ligand charge transfer (MLCT) state, ligand-to-ligand charge transfer (LLCT) state, intraligand charge transfer (ILCT) state, and intraligand (IL) π,π^* state. For example, Wu and co-workers reported the photophysical properties of platinum terpyridyl phenylacetylide complexes bearing amino moieties on phenylacetylide or terpyridyl ligands [29]. Upon protonation, the lowest excited state was switched between LLCT, MLCT, and ILCT, which results in dramatic color change and luminescence intensity change [29]. Yam and co-workers has also developed colorimetric and luminescent pH sensors based on the same mechanism [28]. These results are intriguing; however, the complexes reported are only responsive to acids. To date, no platinum complexes that are sensitive to bases have been reported. To remedy this deficiency, we recently synthesized a new platinum terpyridyl complex (**2**) with dimethylamino substituent on the phenylacetylide ligand and a hydroxylphenyl substituent on the terpyridyl ligand (structure shown in Scheme 1). It is anticipated that upon addition of bases, the hydroxyl group would be deprotonated, which would influence the electron distribution of the complex and thus affect the nature of the lowest excited state. Meanwhile, the presence of the dimethylamino substituent would make this complex sensitive to acids. Such a design would allow for this complex to be a good candidate for acid/base sensor. To demonstrate this, the photophysical properties of this complex, especially the changes of its UV–Vis absorption and emission in acidic and basic solutions, have been systematically investigated.

2. Experimental section

2.1. Synthesis

K_2PtCl_4, trifluoromethanesulfonic acid anhydride, *p*-toluenesulfonic acid, *tetra*-*n*-butylammonium hydroxide 1.0 M solution and all the other reagents were purchased from Aldrich and Alfa Aesar and used without further purification. All solvents are analytical grade and were purchased from VWR International and used

* Corresponding author. Tel.: +1 701 2316254; fax: +1 701 2318831.
E-mail address: Wenfang.Sun@ndsu.edu (W. Sun).

0022-328X/$ - see front matter © 2009 Elsevier B.V. All rights reserved.
doi:10.1016/j.jorganchem.2009.09.015

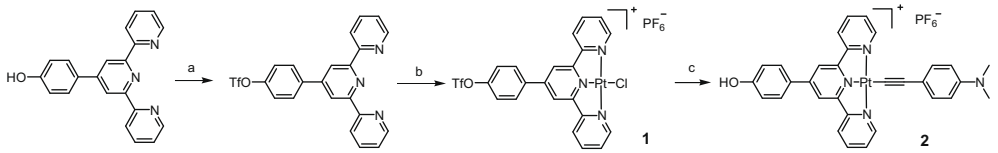

a. $(OTf)_2O$, Pyridine; b. K_2PtCl_4, CH_3CN/H_2O; c. N,N'-dimethylphenylacetylene, KOH, CuI, MeOH.

Scheme 1. Synthetic route of **2**.

without further purification unless otherwise stated. 4′-(*p*-Hydroxylphenyl)terpyridine was synthesized according to the literature procedure [31]. All products were characterized by ^{1}H NMR, elemental analysis, and high resolution MS. ^{1}H NMR spectra were obtained on a Varian 400 MHz or 500 MHz Varian NMR spectrometer. Elemental analyses were conducted by NuMega Resonance Labs, Inc. in San Diego, CA. High resolution MS data were obtained using a Bruker BioTof III spectrometer.

2.2. 4′-(*p*-Trifluoromethylsulfonylphenyl)-terpyridine [32]

4′-(*p*-Hydroxyphenyl)-2,2′:6′,2″-terpyridine (0.82 g, 2.52 mmol) was dissolved in 10 ml dry pyridine. Trifluoromethanesulfonic anhydride (0.83 ml, 4.93 mmol) was slowly added at 0 °C. The resultant mixture was stirred at 0 °C for another 30 min, and then the reaction was warmed to room temperature. The mixture was kept at room temperature for 2 days. After that, the mixture was poured into 200 ml cold water, and solid was separated by filtration. The crude product was purified by recrystallization in ethanol to afford 1.03 g white solid (yield: 95%). ^{1}H NMR (DMSO-d_6, 400 MHz) δ 7.54 (2H, ddd, J = 1.2, 8.7, 12.3 Hz), 7.70 (2H, d, J = 9.0 Hz), 8.05 (2H, dt, J = 1.5, 7.8 Hz), 8.13 (2H, m), 8.67 (2H, d, J = 7.8 Hz), 8.71 (2H, s), 8.75 (2H, m) ppm.

2.3. Complex 1

4′-(*p*-Trifluoromethylsulfonylphenyl)-2,2′:6′,2″-terpyridine (218 mg, 0.48 mmol) was dissolved in 30 ml hot CH_3CN, K_2PtCl_4 (198 mg, 0.48 mmol) was dissolved in 10 ml hot water. These two solutions were added together, and the mixture was heated to reflux for 24 h. After the mixture was cooled to room temperature, yellow solid was separated by filtration, and washed with hexane (50 ml) to give white solid 207 mg (yield: 60%). ^{1}H NMR (DMSO-d_6, 400 MHz) δ 7.85 (2H, d, J = 9.6 Hz), 7.98 (2H, t, J = 6.4 Hz), 8.31 (2H, d, J = 6.8 Hz), 8.55 (2H, dt, J = 8.0, 1.6 Hz), 8.81 (2H, d, J = 7.2 Hz), 8.96 (2H, d, J = 5.6 Hz), 9.02 (2H, s) ppm.

2.4. Complex 2

4-Ethynyl-*N*,*N*-dimethylaniline (14.5 mg, 0.1 mmol) and KOH (11.2 mg, 0.2 mmol) were dissolved in MeOH and stirred at r.t. for 30 min. Complex **1** (61.4 mg, 0.1 mmol) and CuI (1.2 mg, 0.06 mmol) were added. The mixture was purged under Ar for 30 min, and then stirred at r.t. for 18 h. After the reaction, the reaction mixture was concentrated, and ether was added. The black precipitants were separated by filtration. The solid was dissolved in 20 ml MeOH, and 20 ml saturated aqueous solution of NH_4PF_6 was added. The mixture was stirred at r.t. for 3 h, then the dark solid was separated by filtration. The crude product was purified by recrystallization in CH_3CN/Et_2O to give 43.8 mg black solid (yield: 54%). ^{1}H NMR (DMSO-d_6, 400 MHz), 2.97 (6H, s), 6.68 (2H, d, J = 8.0 Hz), 7.02 (2H, d, J = 8.0 Hz), 7.31 (2H, d, J = 7.5 Hz), 7.90 (2H, m), 8.06 (2H, m), 8.49 (2H, m), 8.80 (4H, m), 9.15 (2H, m). Anal. Calc. for $C_{31}H_{25}F_6N_4OPPt$: C, 45.75; H: 3.22; N: 6.97. Found: C, 45.98; H, 3.09; N, 6.92%. HRMS: calcd for $[C_{31}H_{25}N_4OPt^{195}]^+$, 664.1673; found, 664.1676 (100%).

2.5. Photophysical studies

The electronic absorption spectra were recorded on a SHIMADZU 2501 PC UV–Vis spectrophotometer. The emission spectra were recorded on a SPEX Fluorolog-3 fluorometer/phosphorometer. The complex was dissolved in HPLC grade CH_3CN. The emission lifetimes were measured on an Edinburgh LP920 laser flash photolysis spectrometer. Excitation resource was the third-harmonic output (355 nm) of a Quantel Brilliant Q-switched Nd:YAG laser (FWHM pulsewidth was 4.1 ns and the repetition rate was set at 1 Hz). The emission quantum yield was obtained via a comparative method [33], in which a degassed aqueous solution of $[Ru(bpy)_3]Cl_2$ (Φ_{em} = 0.042 at 436 nm excitation) was used as the reference [34].

3. Results and discussion

3.1. Electronic absorption

The electronic absorption spectrum of **2** is shown in Fig. 1. Within the concentration range studied (4.8×10^{-6}–9.6×10^{-5} mol/L), the absorption of **2** obeys Beer–Lambert's law, indicating no ground-state aggregation. Complex **2** exhibits intense UV absorption below 370 nm, which can be attributed to the π,π^* transitions within the terpyridyl and phenylacetylide ligands. In addition, two broad absorption bands are observed in the visible spectral region. With reference to the UV–Vis absorption of other platinum complexes reported in the literature [28], the absorption band at 380–460 nm can be assigned to the $d\pi(Pt) \rightarrow \pi^*$(terpyr-

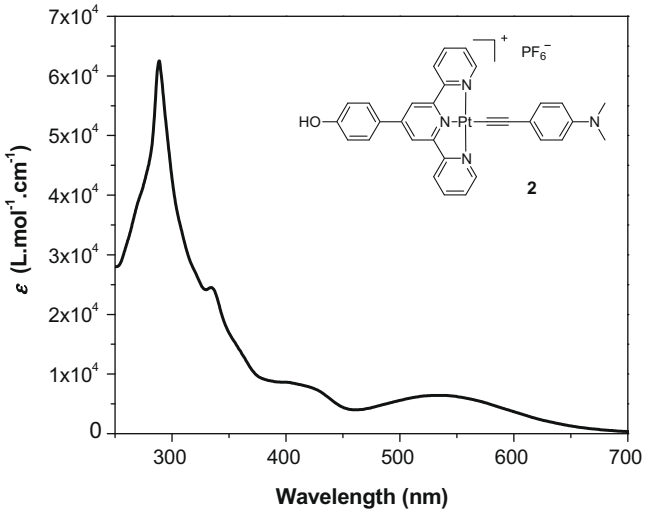

Fig. 1. UV–Vis absorption spectrum of **2** in CH_3CN.

idyl) ^{1}MLCT transition; while the lowest absorption band from 460 to 670 nm is attributed to the $\pi[N(CH_3)_2PhC{\equiv}C] \rightarrow \pi^*$(terpyridyl) ^{1}LLCT transition [28,29]. The assignment of the low-energy absorption bands to charge transfer transitions is supported by the negative solvatochromic effect of **2** in solvents with different polarities, *i.e.* these bands shift to longer wavelengths in less polar solvents such as CH_2Cl_2 and THF compared to those in more polar solvents like CH_3OH and CH_3CN (shown in Fig. 2). This implies a more polar ground state than the excited state. The charge transfer nature of the lowest-energy band is further evident by the dramatic blue-shift of this band upon protonation by acid, which significantly decreases the electron-donating ability of the dimethylaminophenylacetylide ligand and moves the ^{1}LLCT to a much higher energy. This point will be discussed further in Section 3.3.

3.2. Photoluminescence

Distinct from the nonemissive platinum terpyridyl complexes with dialkylamino substituent reported in the literature [28,29], **2** exhibits dual emission in CH_3CN at r.t. when excited at 334 nm, and the relative emission intensity is concentration-dependent. As shown in Fig. 3, at lower concentrations (4.8×10^{-6} and 9.6×10^{-6} mol/l), the emission at 445 nm dominates. At higher concentrations (4.8×10^{-5} and 9.6×10^{-5} mol/l), the emission at 445 nm diminishes, while the emission at *ca.* 560 nm becomes dominant. When excited at 411 nm, only the 560 nm band is observed. The lifetimes of these two emission bands are quite distinct. The emission band at 445 nm is short-lived, with a lifetime that is too short to be measured on our spectrometer (<5 ns). In contrast, the intrinsic lifetime for the emission at 560 nm is approximately 830 ns. This implies that the origins of these two emission bands are different. This notion is confirmed by the excitation spectra measurement. When monitored at the 445 nm emission band, the excitation band appears at *ca.* 260–400 nm, which coincides with the $^1\pi,\pi^*$ transition in the UV–Vis spectrum. When monitored at the 560 nm emission band, the excitation band maximum occurs at *ca.* 430 nm, which lies in the ^{1}MLCT band region. In view of the different excitation spectra and different lifetimes of these two emission bands, we conclude that these two emission bands emanate from different excited states. The emission at 445 nm likely emanates from the intraligand $^1\pi,\pi^*$ excited state, while the 560 nm band could originate from a triplet excited state due to the much large Stokes shift (~130 nm) and the significantly long lifetime. In addition, this emission band is very sensitive to oxygen. In deaerated solution, the emission intensity is several orders of magnitude higher than that in aerated solution. The emission quantum yield for the 560 nm band is measured to be 0.0048 in deaerated CH_3CN solution. The dual emission was also reported by Wong and co-workers for a class of trifunctional Pt(II) cyclometallated platinum complexes [35].

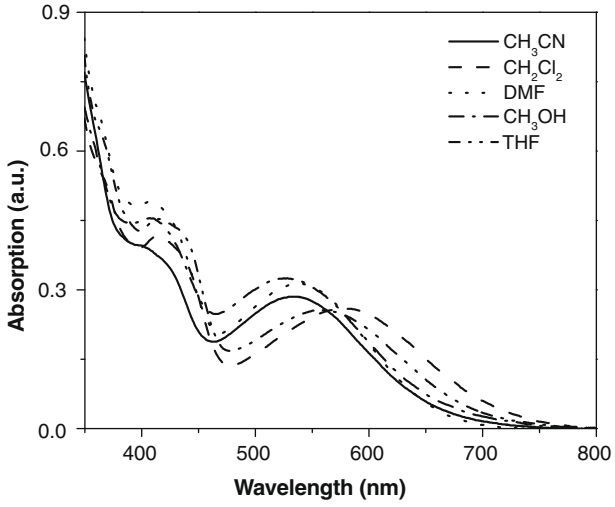

Fig. 2. UV–Vis absorption spectra of **2** in different solvents in 1-cm cuvette ($c = 4.8 \times 10^{-5}$ mol/l).

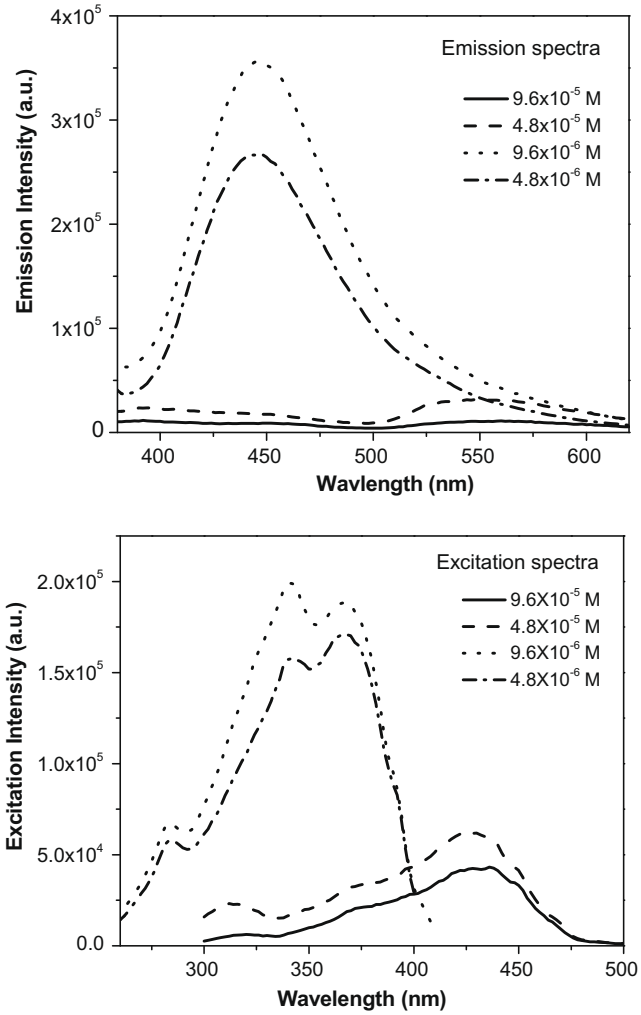

Fig. 3. Concentration-dependent room temperature emission and excitation spectra of **2**. For emission spectra measurements, the excitation wavelength was 334 nm.

Considering the nature of the emitting triplet excited state, it could admix the ^{3}MLCT and $^3\pi,\pi^*$ configurations. This notion can be supported by the following pieces of evidences: (1) As shown in Fig. 4, this band exhibits insignificant solvent effect, which is a characteristic of the π,π^* transition. (2) Although the emission band shows somewhat structures, it is quite broad. The broad emission profile indicates the involvement of charge transfer character in the emitting state, which should be the ^{3}MLCT state. (3) The presence of oxygen in solution not only quenches the emission intensity but also changes the emission band apex. As displayed in Fig. 5, the apex shifts from 558 nm in an aerated solution to 530 nm after degassing. This implies that the broad emission originates from two configurationally distinct emitting states that lie in close proximity but show different sensitivity to oxygen. However, the emission decays symmetrically with time in deaerated solution, which is evidenced by the time-resolved emission spectra and the lifetimes measured at 530 nm and 558 nm are almost

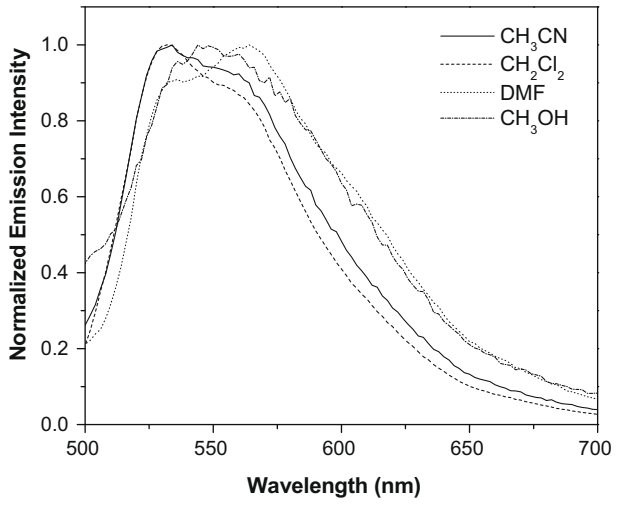

Fig. 4. Normalized emission spectra of **2** in different solvents ($c = 4.8 \times 10^{-5}$ mol/l). $\lambda_{ex} = 411$ nm.

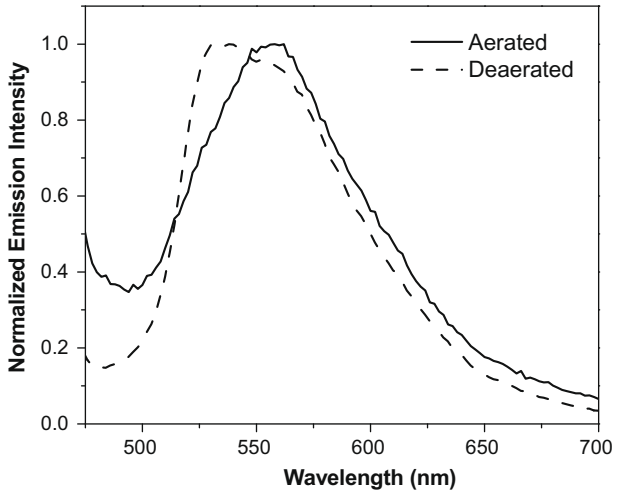

Fig. 5. Normalized emission spectra of **2** in aerated and deaerated CH_3CN solution. $\lambda_{ex} = 411$ nm.

the same (the intrinsic lifetime obtained at 530 nm is 815 ns and 833 ns at 558 nm). (4) The mixture of the ^{3}MLCT and $^3\pi,\pi^*$ configurations is further evidenced by base titration that will be discussed in Section 3.3. As shown in Fig. 7, upon base titration, the emission at 558 nm gradually decreases, while the emission at 530 nm is much less affected by base. As will be discussed in detail later, upon addition of base, the low-lying excited states switch from MLCT/LLCT to LLCT/ILCT (intraligand charge transfer), which consequently decreases the ^{3}MLCT emission with the $^3\pi,\pi^*$ emission largely unaffected. In addition to the aforementioned evidences, the mixture of ^{3}MLCT with $^3\pi,\pi^*$ characters in the emitting state has been proposed by McMillin and co-workers for 4′-substituted Pt(trpy)Cl complexes bearing aryl groups [36] and by Castellano and co-workers for $[Pt(4'\text{-}C{\equiv}CR\text{-}tpy)Cl]^+$ complexes [37].

Another point worthy of mention is that the concentration-dependent behaviors of these two emission bands are different. The emission band at 445 nm is completely quenched when the concentration is increased to 4.8×10^{-5} mol/l, while the emission at 560 nm is still apparent. The rapid quenching of the 445 nm band could possibly be due to the formation of nonemissive ground-state aggregates, the inner-filter effect, or the self-quenching effect. The formation of ground-state aggregates could be easily excluded due to the fact that the UV–Vis absorption obeys Beer–Lambert's law from 4.8×10^{-6} to 9.6×10^{-4} mol/l. In view of the larger extinction coefficients of the electronic absorption at 560 nm than that at 445 nm, the inner-filter effect could not be the dominant contributor, either. This is because if the inner-filter effect dominates, the emission at 560 nm should be quenched more quickly than the band at 445 nm. Therefore, the rapid

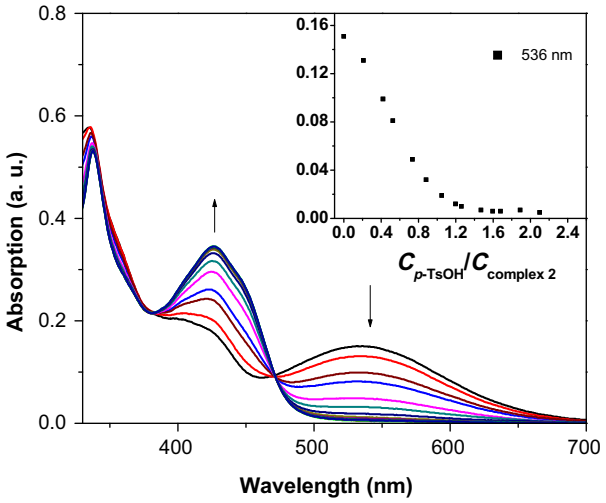

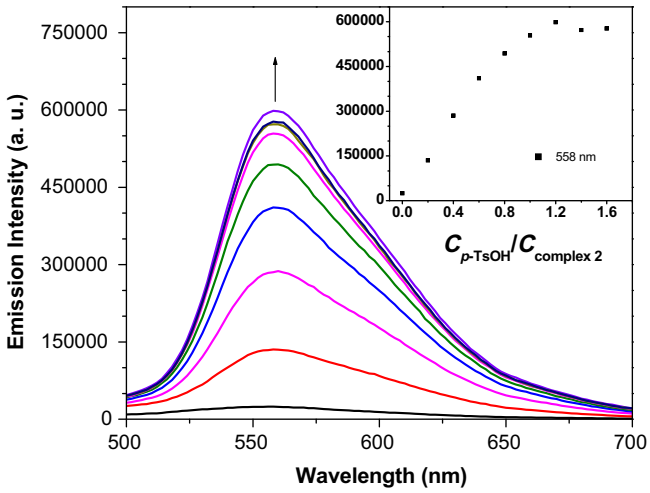

Fig. 6. UV–Vis absorption spectra and emission spectra at room temperature of **2** in CH_3CN (5.0×10^{-5} mol/l) with addition of *p*-TsOH (1.5×10^{-2} mol/l).

Fig. 7. Complex **2** in CH_3CN (5.0×10^{-5} mol/l, middle) with various *p*-TsOH concentration (left 1 to left 3: 5.6×10^{-5}, 3.9×10^{-5}, 3.4×10^{-5} mol/l); and various *n*-Bu_4NOH concentration (left 4 to right): 0.6×10^{-5}, 1.3×10^{-5}, 2.3×10^{-5} mol/l.

quenching of the 445 nm band should be mainly attributed to the self-quenching effect, although the inner-filter effect could also contribute. Unfortunately, confirmation of the self-quenching effect could not be conducted due to the limitation of our spectrometer's resolution (<5 ns). Nevertheless, the more rapid quenching of the 445 nm band than the 560 nm band suggests that the self-quenching constant of the $^1\pi,\pi^*$ state is larger than that of the ^{3}MLCT/$^3\pi,\pi^*$ state.

For the 560 nm emission band, the emission intensity also decreases with increased concentration. The lifetime measurement of different-concentration solutions revealed that the emission lifetime becomes shorter at higher concentrations. The lifetime measured at 5×10^{-6}, 1×10^{-5}, 3×10^{-5} and 6×10^{-5} mol/l is 979, 597, 481 and 390 ns, respectively. Extrapolation of the intercept and slope from the plot of decay rate constant ($k_{obs.}$) vs. concentration gives rise to the intrinsic lifetime and self-quenching constant of 833 ns and 2.4×10^{10} l mol^{-1} s^{-1}, respectively. The lifetimes monitored at 530 nm for different concentrations are similar to those obtained at 560 nm, and a similar self-quenching constant is observed (the results are shown in Table 1).

3.3. Acid and base titration

Yam and co-workers reported that platinum terpyridyl complexes containing dimethylamino substituent(s) exhibit drastic color change and the emission was "turned on" upon protonation [28,29]. These changes were attributed to the switching of the excited state from LLCT/ILCT to MLCT after protonation. Because complex **2** also possess a dimethylamino substituent on the phenylacetylide ligand and the lowest-energy absorption band is assigned to the ^{1}LLCT transition, it is expected that a similar change of the nature of the lowest-energy excited state from LLCT to MLCT would occur. To demonstrate this, the electronic absorption and emission spectra of **2** was monitored upon addition of *p*-TsOH in CH_3CN. The acid titration was performed in CH_3CN solution because **2** is not water-soluble. As shown in Fig. 6, the ^{1}LLCT band at *ca.* 536 nm gradually decreases after addition of acid, accompanied by the increase of the ^{1}MLCT absorption band at *ca.* 425 nm. An isosbestic point at 472 nm is formed during the titration, indicating that only two interconverting species are present in the solution. In accordance with this spectroscopic change, the color of the solution changes from the original purple color to yellow (Fig. 7). The drastic change of the UV–Vis spectrum of **2** with addition of *p*-TsOH should be attributed to the protonation of the dimethylamino substituent, which dramatically lowers the phenylacetylide-based molecular orbital and moves the Pt-based orbital as the HOMO. Consequently, the lowest excited state is switched from ^{1}LLCT to ^{1}MLCT. The change of the nature of the lowest excited state also influences the emission intensity drastically. As shown in Fig. 6, upon addition of *p*-TsOH, the emission intensity of **2** at 558 nm gradually increases. When the acid concentration is increased to 1 equiv., the emission intensity reaches the maximum point (20 times higher than the original intensity). The lifetime of the emission monitored at 558 nm in the presence of excess amount of *p*-TsOH is 260 ns, which is shorter than that of the original ^{3}MLCT/$^3\pi,\pi^*$ emission from **2** as discussed in the previous section. The lifetime variation reflects the mixing of different amount of ^{3}MLCT and $^3\pi,\pi^*$ characters before and after protonation. The shortened lifetime after protonation suggests more contribution from the charge transfer state. This further confirms that the emissive ^{3}MLCT state becomes the lowest excited state after protonation of **2**, which is consistent with what have been reported by Yam and co-workers [28] and Wu and co-workers [29]. The same change of the UV–Vis spectrum and the emission intensity was observed upon acidification using HCl or other common organic acids such as HBF_4.

Complex **2** is also responsive to bases. With addition of $(n\text{-Bu})_4$NOH to CH_3CN solution of **2**, both the electronic absorption spectrum and the emission intensity of **2** change (shown in Fig. 8). The change of the UV–Vis spectrum of **2** is stepwise: with addition of 0–0.5 equiv. $(n\text{-Bu})_4$NOH, the lowest-energy absorption band maximum bathochromically shifts from 536 to 594 nm, accompanied by the decrease of the absorption around 425 nm, and an isosbestic point appears at 439 nm; with addition of 0.6–1.0 equiv. $(n\text{-Bu})_4$NOH, the absorption at 594 nm continuously increases and a new isosbestic point occurs at 494 nm. No further change was observed upon addition of excess amount of $(n\text{-Bu})_4$NOH. Corresponding to this spectral change, the color of the solution changes from purple to blue (illustrated in Fig. 7). On the other hand, addition of $(n\text{-Bu})_4$NOH gradually quenches the emission at 558 nm, while the emission at 530 nm is essentially unaffected. After addition of 0.5 equiv. $(n\text{-Bu})_4$NOH, no further change in the emission spectrum is observed.

Table 1
Photophysical parameters of **2** at room temperature in CH_3CN.

λ_{abs}/nm (ε/M^{-1} cm^{-1})	λ_{em}/nm (τ_{em}/ns; Φ_{em}; k_q[a]/M^{-1} s^{-1})
289 (62 520), 334 (24 500), 407 (8460), 536 (6440)	445, 530 (815; -; 3.25×10^{10}), 558 (833; 0.0048; 2.42×10^{10})

[a] Self-quenching constant, obtained from the slope of the plot $k_{obs} = 1/\tau_0 + k_q[C]$.

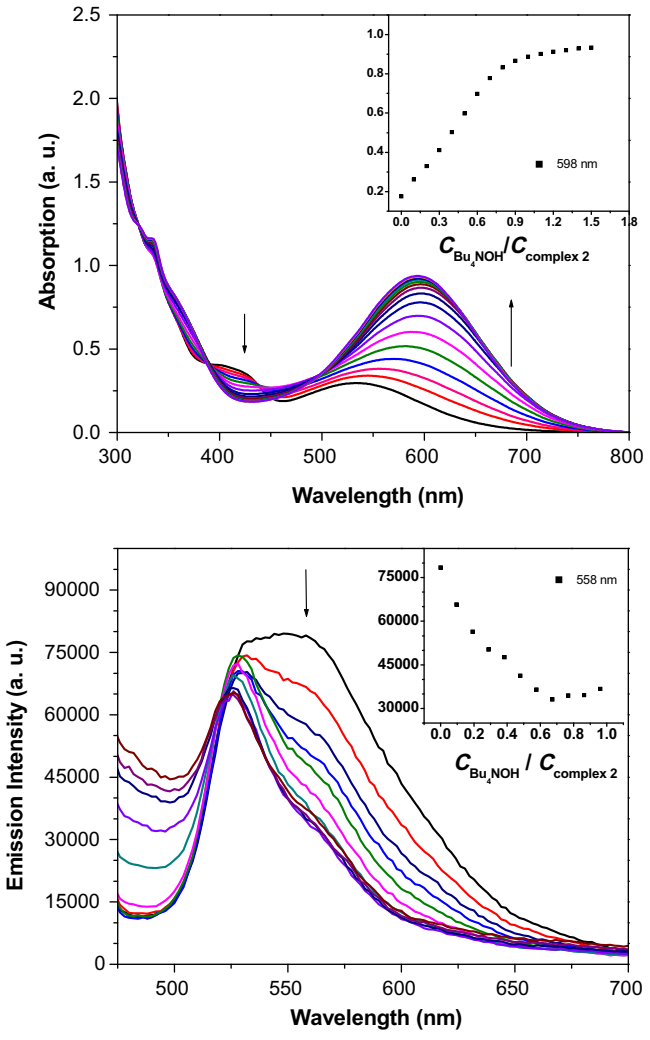

Fig. 8. UV–Vis absorption and emission spectra of **2** in CH_3CN (5.0×10^{-5} mol/l) with addition of n-Bu_4NOH (1.5×10^{-2} mol/l).

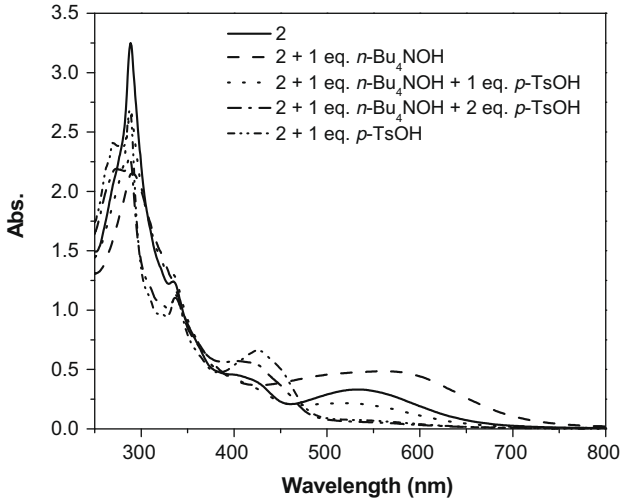

Fig. 9. UV–Vis absorption spectra of **2** in CH_3CN (5.0×10^{-5} mol/l) with addition of n-Bu_4NOH (1.5×10^{-2} mol/l) and p-TsOH (1.5×10^{-2} mol/l).

The bathochromic shift of the lowest-energy absorption band in the UV–Vis spectrum and the quench of the emission at 558 nm can be rationalized as following: upon addition of (n-Bu)$_4$NOH, the OH substituent at the terpyridyl ligand is deprotonated, which increases the electron density on the phenyl ring. This would destabilize the molecular orbital of the phenoxide and move it up as the HOMO. In such a case, the intraligand charge transfer state (^{1}ILCT) between the phenoxide-based HOMO and the terpyridine-based LUMO becomes the lowest excited state, which appears at 594 nm and partially overlaps with the ^{1}LLCT absorption at *ca.* 536 nm. Thus, the broad band from 450 to 750 nm after deprotonation can be assigned as a mixture of ^{1}ILCT and ^{1}LLCT. The appearance of the low-lying nonemissive ILCT state adds an additional decay path for the emitting MLCT state and thus quenches the ^{3}MLCT emission at 558 nm more rapidly. In contrast, the $^3\pi,\pi^*$ state remains intact energetically as evidenced in Fig. 8, where the emission at 530 nm has essentially no change with deprotonation.

A point worthy of mention is that the acid-induced changes in UV–Vis and emission spectra are essentially reversible. After addition of 1 equiv. of n-Bu_4NOH to the acidified CH_3CN solution of **2** with 1 equiv. of p-TsOH, both the UV–Vis and emission spectra essentially recovered to their original forms. However, as shown in Fig. 9, the base induced change is not completely reversible upon addition of an equal amount of acid to the basicified solution. Only when one more equivalent of p-TsOH was added, the UV–Vis and emission spectra became almost identical to the acidified solution from the original form of **2** with 1 equiv. of p-TsOH. This phenomenon could be due to the competition between the phenoxide anionic component and the dimethylamino substituent when 1 equiv. of acid was added. After addition of 2 equiv. of acid, both the phenoxide anion and the dimethylamino substituent are protonated, which gives rise to the similar UV–Vis and emission spectra as those for the acidified solution from the original form of **2**.

4. Conclusions

The platinum complex (**2**) with both dimethylamino substituent and hydroxylphenyl substituent on its ligands exhibits a drastic color change from yellow in acidic solution to blue in basic CH_3CN solutions. Its emission at 558 nm is significantly enhanced in acidic solution, and is quenched in basic solution. These dramatic changes are caused by the change of the electron density on the ligands upon protonation of the dimethylamino substituent in acidic solution and deprotonation of the hydroxyl group in basic solution, which in turn changes the nature of the lowest excited state. In acidic solution, the lowest excited state is switched from LLCT to MLCT; while in basic solution, it is altered from LLCT to ILCT. The dramatic color change and emission intensity change make **2** a promising candidate as a chromogenic and luminescent acid/base sensor in organic solvent. With further modification of **2** to become water-soluble, **2** could potentially be used as a pH sensor.

Acknowledgments

This research was supported by the National Science Foundation (CAREER CHE-0449598). We are grateful to North Dakota State EPSCoR (ND EPSCoR Instrumentation Award) for support.

References

[1] W. Lu, B.-X. Ma, M.C.W. Chan, Z. Hui, C.-M. Che, N. Zhu, S.-T. Lee, J. Am. Chem. Soc. 126 (2004) 4958.
[2] H. Yersin, D. Donges, W. Humbs, J. Strasser, R. Sitters, M. Glasbeek, Inorg. Chem. 41 (2002) 4915.
[3] J. Brooks, Y. Babayan, S. Lamansky, P.I. Djurovich, I. Tsyba, R. Bau, M.E. Thompson, Inorg. Chem. 41 (2002) 3055.
[4] J.C. Shi, H.Y. Chao, W.F. Fu, S.M. Peng, C.M. Che, J. Chem. Soc., Dalton Trans. 18 (2000) 3128.
[5] L. Chassot, A. von Zelewsky, D. Sandrini, M. Maestri, V. Balzani, J. Am. Chem. Soc. 108 (1986) 6084.
[6] M. Maestri, D. Sandrini, V. Balzani, L. Chassot, P. Jolliet, A. von Zelewsky, Chem. Phys. Lett. 122 (1985) 375.
[7] W.-Y. Wong, Z. He, S.-K. So, K.-L. Tong, Z. Lin, Organometallics 24 (2005) 4079.
[8] G.-J. Zhou, X.-Z. Wang, W.-Y. Wong, X.-M. Yu, H.-S. Kwok, Z. Lin, J. Organomet. Chem. 692 (2007) 3461.
[9] C.-L. Ho, W.-Y. Wong, B. Yao, Z. Xie, L. Wang, Z. Lin, J. Organomet. Chem. 694 (2009) 2735.
[10] S. Chakraborty, T.J. Wadas, H. Hester, C. Flaschenreim, R. Schmehl, R. Eisenberg, Inorg. Chem. 44 (2005) 6284.
[11] S. Chakraborty, T.J. Wadas, H. Hester, C.R. Schmehl, R. Eisenberg, Inorg. Chem. 44 (2005) 6865.
[12] W.-Y. Wong, X.Z. Wang, Z. He, A.B. Djurisic, C.-T. Yip, K.-Y. Cheung, H. Wang, C.S.K. Mak, W.-K. Chan, Nat. Mater. 6 (2007) 521.
[13] W.-Y. Wong, Macromol. Chem. Phys. 209 (2008) 14.
[14] W. Sun, Z.-X. Wu, Q.-Z. Yang, L.-Z. Wu, C.-H. Tung, Appl. Phys. Lett. 82 (2003) 850.
[15] W. Sun, F. Guo, Chin. Opt. Lett. S3 (2005) S34.
[16] F. Guo, W. Sun, J. Phys. Chem. B 110 (2006) 15029.
[17] T.M. Pritchett, W. Sun, F. Guo, B. Zhang, M.J. Ferry, J.E. Rogers-Haley, W. Shensky, A.G. Mott, Opt. Lett. 33 (2008) 1053.
[18] G.-J. Zhou, W.-Y. Wong, Z. Lin, C. Ye, Angew. Chem., Int. Ed. Engl. 45 (2006) 6189.
[19] G. Zhou, Funct. Mater. 19 (2009) 531.
[20] D. Zhang, L.-Z. Wu, Q.-Z. Yang, X.-H. Li, L.-P. Zhang, C.-H. Tung, Org. Lett. 5 (2003) 3221.
[21] Y. Yang, D. Zhang, L.-Z. Wu, B. Chen, L.-P. Zhang, C.-H. Tung, J. Org. Chem. 69 (2004) 4788.
[22] X.-H. Li, L.-Z. Wu, L.-P. Zhang, C.-H. Tung, C.M. Che, Chem. Commun. 21 (2001) 2280.
[23] K. Feng, R.-Y. Zhang, L.-Z. Wu, B. Tu, M.-L. Peng, L.-P. Zhang, D. Zhao, C.-H. Tung, J. Am. Chem. Soc. 128 (2006) 14685.
[24] Q.-Z. Yang, L.-Z. Wu, H. Zhang, B. Chen, Z.-X. Wu, L.-P. Zhang, Z.-H. Tung, Inorg. Chem. 43 (2004) 5195.
[25] L.Z. Wu, T.C. Cheung, C.M. Che, K.K. Cheung, M.H. Lam, Chem. Commun. 10 (1998) 1127.
[26] K.-H. Wong, M.C.-W. Chan, C.M. Che, Chem. Eur. J. 5 (1999) 2845.
[27] S.C.F. Kui, S.S.-Y. Chui, C.-M. Che, N. Zhu, J. Am. Chem. Soc. 128 (2006) 8297.
[28] K.M. Wong, W.-S. Tang, X.-X. Lu, N. Zhu, V.W.-W. Yam, Inorg. Chem. 44 (2005) 1492.
[29] X. Han, L.-Z. Wu, G. Si, J. Pan, Q.-Z. Yang, L.-P. Zhang, C.-H. Tung, Chem. Eur. J. 13 (2007) 1231.
[30] K.M.-C. Wong, W.-S. Tang, B.W.-K. Chu, N. Zhu, V.W.-W. Yam, Organometallics 23 (2004) 3459.
[31] D.W. Yoo, S.K. Yoo, C. Kim, J.K. Lee, J. Chem. Soc., Dalton Trans. (2002) 3931.
[32] K.T. Potts, D. Konwar, J. Org. Chem. 56 (1991) 4815.
[33] J.N. Demas, G.A. Crosby, J. Phys. Chem. 75 (1971) 991.
[34] J. Van Houten, R.J. Watts, J. Am. Chem. Soc. 98 (1976) 4853.
[35] Z. He, W.-Y. Wong, X. Yu, H.-S. Kwok, Z. Lin, Inorg. Chem. 45 (2006) 10922.
[36] J.F. Michalec, S.A. Bejune, D.G. Cuttell, G.C. Summerton, J.A. Gertenbach, J.S. Field, R.J. Haines, D.R. McMillin, Inorg. Chem. 40 (2001) 2193.
[37] M.L. Muro, F.N. Castellano, Dalton Trans. (2007) 4659.